Possible Search for η-Mesic Nuclei at GRAAL

A.I. Lebedev, A.I. L'vov, L.N. Pavlyuchenko, G.A. Sokol (LPI)

(partly based on a previous proposal for GRAAL -
nucl-ex/0306011)

ηN and ηA interaction

Experimental information on ηN interaction mostly comes from

$\pi N \to \eta N$ and $\gamma N \to \eta N$

in comparison with

$\pi N \to \pi N$ and $\gamma N \to \pi N$.

Coupled-channel analysis by Green, Wycech. PRC 71, 014001(2005)

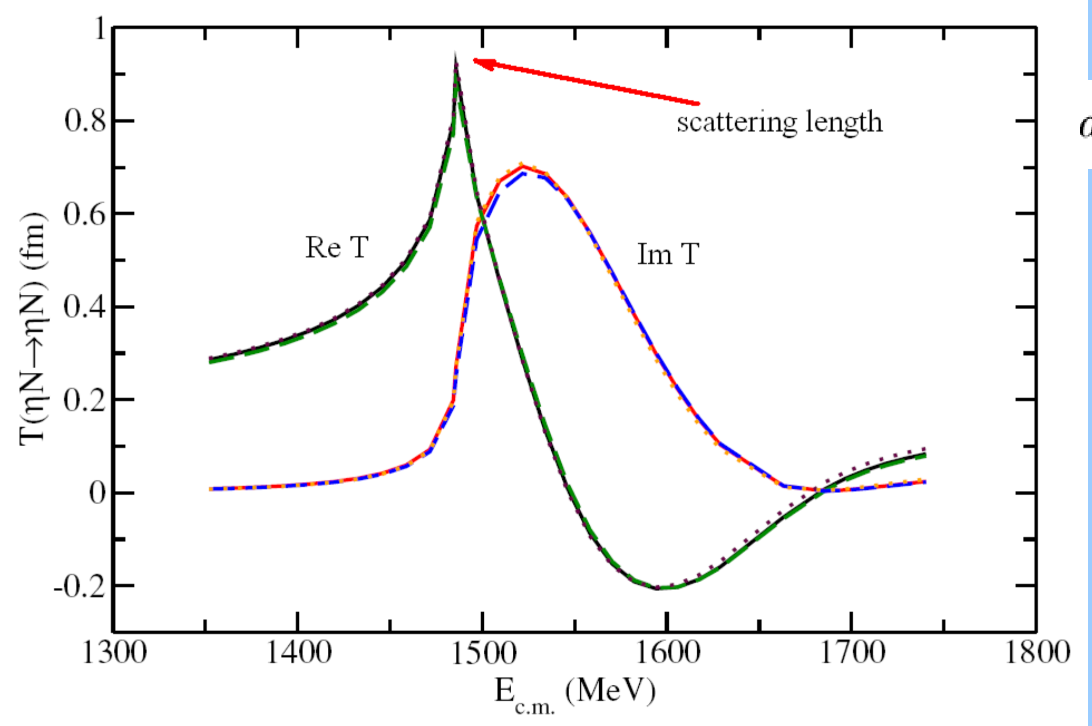

$$a_{\eta N} = (0.91 \pm 0.06) + i\,(0.27 \pm 0.02)\ \text{fm}$$

Though in literature there are Re $a_{\eta N}$ from -0.15 to +1.05 fm and Im $a_{\eta N}$ from 0.15 to 0.49 fm.

Prominent feature of ηN interaction is excitation of the $S_{11}(1535)$ resonance near threshold.

TABLE I. η-nucleon s-wave scattering lengths $a_{\eta N}$.

$a_{\eta N}$ (fm)	Formalism or reaction	Reference
$0.270+0.220i$	Isobar model	Bhalerao and Liu [2]
$0.280+0.190i$	Isobar model	Bhalerao and Liu [2]
$0.281+0.360i$	Photoproduction of η	Krusche [23]
$0.430+0.394i$		Krusche [23]
$0.579+0.399i$		Krusche [23]
$0.476+0.279i$	Electroproduction of η	Tiator *et al.* [22]
$0.500+0.330i$	$pd \rightarrow {}^3\mathrm{He}\, e\, \eta$	Wilkin [24]
$0.510+0.210i$	Isobar model	Sauermann *et al.* [14]
$0.550+0.300i$		Sauermann *et al.* [14]
$0.620+0.300i$	Coupled T matrices	Abaev and Nefkens [16]
$0.680+0.240i$	Effective Lagrangian	Kaiser *et al.* [17]
$0.750+0.270i$	Coupled K matrices	Green and Wycech [12]
$0.870+0.270i$	Coupled K matrices	Green and Wycech [13]
$1.050+0.270i$		Green and Wycech [13]
$0.404+0.343i$	Coupled T matrices	Batinić *et al.* [18]
$0.876+0.274i$		Batinić and Švarc [19]
$0.886+0.274i$		Batinić and Švarc [19]
$0.968+0.281i$		Batinić *et al.* [20]
$0.980+0.370i$	Coupled T matrices	Arima *et al.* [21]

Owing to Re $a_{\eta N} > 0$ there is an attraction between a slow η and nuclear matter.

First-order optical potential: $$2m_\eta^* V_{\eta A}(r; E_\eta = 0) = -4\pi\rho(r) a_{\eta N}\left(1 + \frac{m_\eta}{m_N}\right)$$

Actually the attraction is expected to be less due nucleon Fermi motion, broadening the $S_{11}(1535)$ resonance, and some other medium effects.

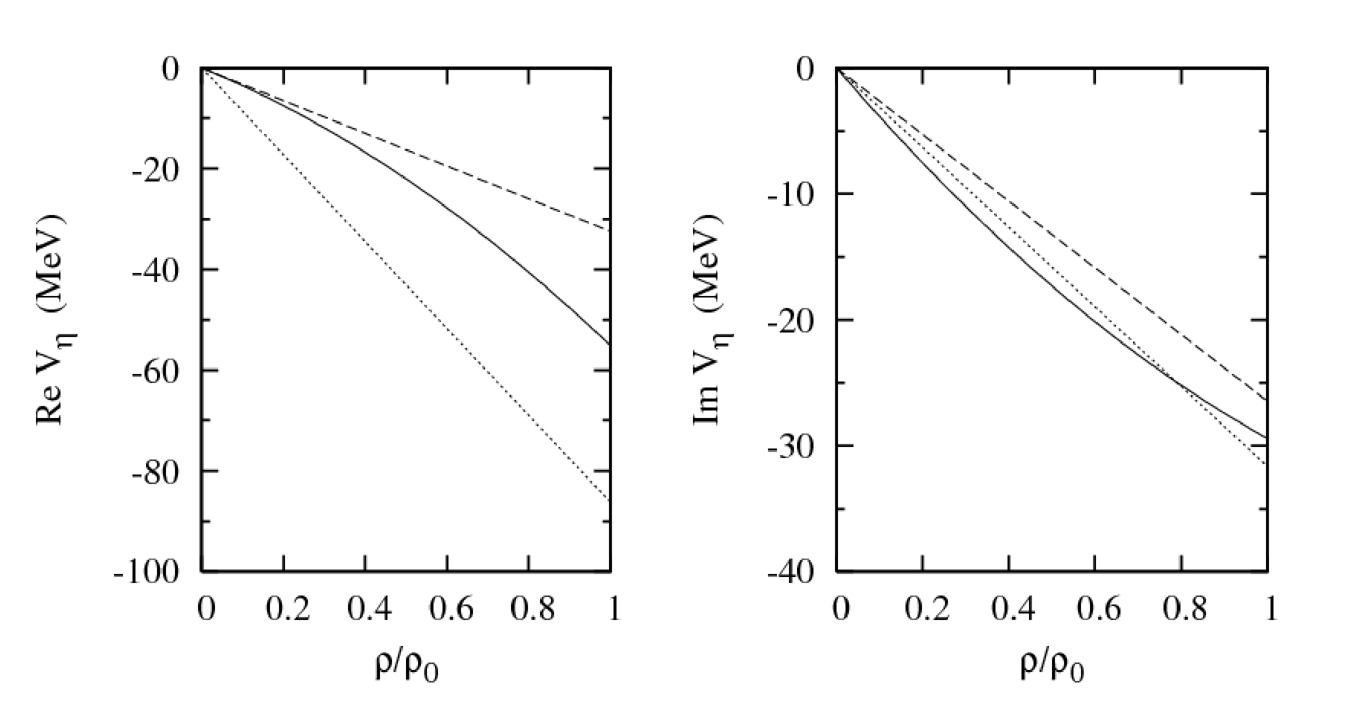

Dashed line: $a_{\eta N}$ = 0.27 + *i* 0.22 fm Bhalerao, Liu, PRL 54, 865(1985)
Dotted line: $a_{\eta N}$ = 0.717 + *i* 0.263 fm Green, Wycech, PRC 55, R2167(1997)
Solid line: chiral unitary approach Inoue, Oset, NPA 710, 354(2002)

η-mesic nuclei

Bound states of η in nuclei   Haider, Liu, PRC 34, 1845(1986)

Depending on the strength of the optical ηN potential such bound states exist at A>11 (Haider, Liu, 1986) or even at A=3 and 2 (Ueda, PRL 66, 297(1991)).

Q. HAIDER AND L. C. LIU   PHYS REV C **66**, 045208 (2002)

TABLE II. Binding energies and half-widths (both in MeV) of η-mesic nuclei given by the full off-shell calculation. The solutions were obtained with the ηN interaction parameters determined from the πN phase shifts of Arndt *et al.* (Ref. [38]). No bound state solutions of Eq. (1) were found for $A < 12$.

Nucleus	Orbital $(n\ell)$	$\epsilon_\eta + i\Gamma_\eta/2$
^{12}C	$1s$	$-(1.19+3.67i)$
^{16}O	$1s$	$-(3.45+5.38i)$
^{26}Mg	$1s$	$-(6.39+6.60i)$
^{40}Ca	$1s$	$-(8.91+6.80i)$
^{90}Zr	$1s$	$-(14.80+8.87i)$
	$1p$	$-(4.75+6.70i)$
^{208}Pb	$1s$	$-(18.46+10.11i)$
	$2s$	$-(2.37+5.82i)$
	$1p$	$-(12.28+9.28i)$
	$1d$	$-(3.99+6.90i)$

C. García-Recio et al. / Phys Lett B 550 (2002) 47

Table 1
$(B, -\Gamma/2)$ for η–nucleus bound states calculated with the energy-dependent potential

	^{12}C	^{24}Mg
$1s$	$(-9.71, -17.5)$	$(-12.57, -16.7)$
$1p$		

Table 2
$(B, -\Gamma/2)$ for η–nucleus bound states calculated with the energy-independent potential

	^{12}C	^{24}Mg
$1s$	$(-17.71, -25.42)$	$(-22.69, -25.78)$
$1p$		

(mean-field [local density] calculation)

S. A. RAKITYANSKY *et al.* PHYSICAL REVIEW C VOLUME 53 R2043 1996

$a_{\eta N} = (g 0.55 + i g' 0.30)$ fm

TABLE II. The parameter g generating the η-nucleus amplitude poles $p_0 = \sqrt{2\mu E_0}$ on the diagonal for the three values of the range parameter α and $g' = 1$.

	g	p_0 (fm^{-1})	E_0 (MeV)	α (fm^{-1})
ηd	1.6536	$-0.32527 + i0.32527$	$-i9.7026$	2.357
	1.5605	$-0.33541 + i0.33541$	$-i10.317$	3.316
	1.5260	$-0.33670 + i0.33670$	$-i10.397$	7.617
ηt	1.3624	$-0.33515 + i0.33515$	$-i9.5266$	2.357
	1.3055	$-0.35190 + i0.35190$	$-i10.503$	3.316
	1.2436	$-0.35186 + i0.35186$	$-i10.500$	7.617
$\eta ^3\mathrm{He}$	1.3306	$-0.34034 + i0.34034$	$-i9.8239$	2.357
	1.2171	$-0.36267 + i0.36267$	$-i11.155$	3.316
	1.1421	$-0.37631 + i0.37631$	$-i12.010$	7.617
$\eta ^4\mathrm{He}$	0.86222	$-0.20641 + i0.20641$	$-i3.4679$	2.357
	0.80813	$-0.26522 + i0.26522$	$-i5.7255$	3.316
	0.79578	$-0.35215 + i0.35215$	$-i10.094$	7.617

(microscopic few-body calculation)

Birth, Life, and Death of η-mesic nuclei

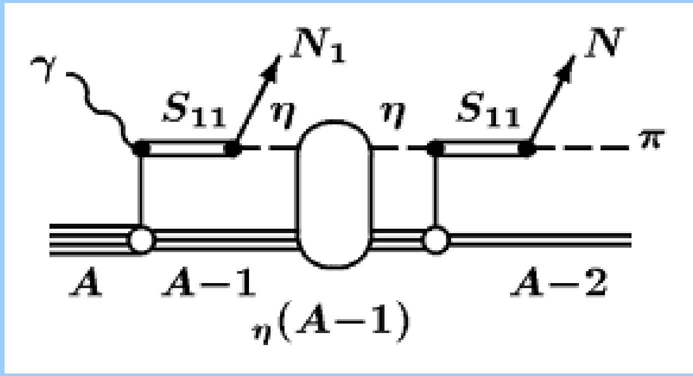

Signature of the eta-mesic nucleus is a peak in the energy distribution of decay products (like πN or NN) or in the energy transfer ($E_\gamma - E_{N1}$).

Both the quantities are measures of the energy of η in medium.

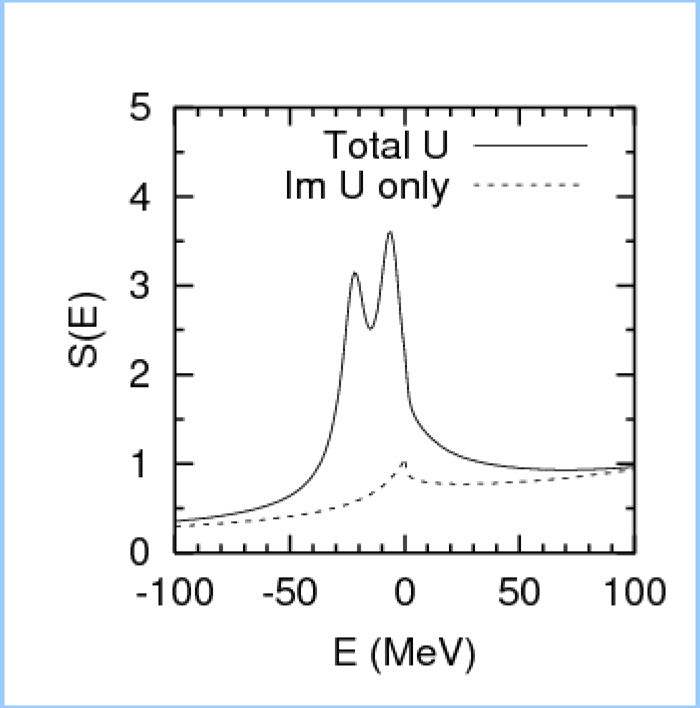

Spectral function for ^{12}C vs the energy of η (a rectangular-well optical potential)

Photoproduction of η-mesic nuclei was considered by Lebedev, Tryasuchev (1989, 1991), Kohno, Tanabe (1989), Tryasuchev (1999, 2001).

Below some Lebedev's and Tryasuchev's results are quoted (mostly from Phys.Part.Nucl. 30, 606(1999); Phys.At.Nucl. 64, 346(2001))

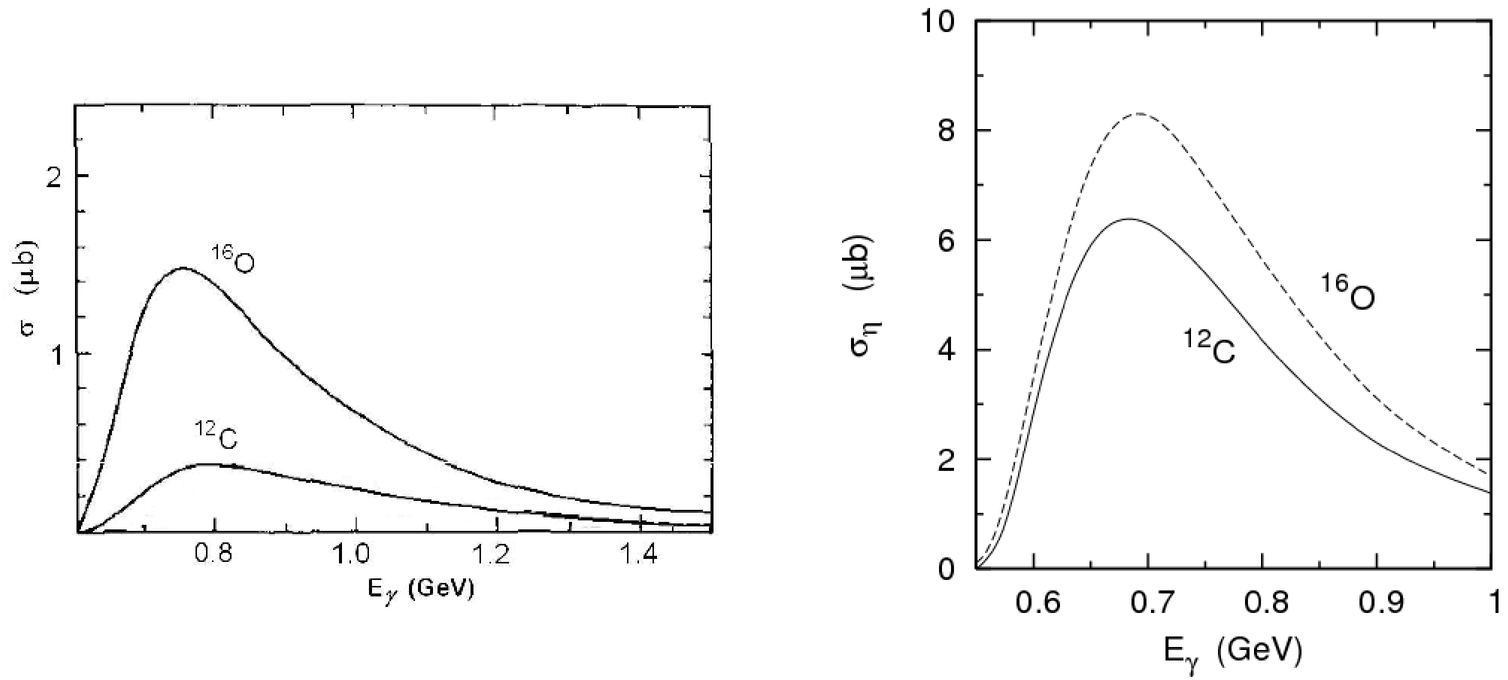

FIG. 4: Total cross section of η-mesic nucleus photoproduction with a proton knock-out, Eq. (5) for the nuclear targets ^{12}C and ^{16}O. Left: Ref. [20] ($a_{\eta N} = 0.27 + i \cdot 0.22$ fm). Right: Ref. [31] ($a_{\eta N} = 0.717 + i \cdot 0.263$ fm); shown lines are obtained by summing partial cross sections shown in Figs. 3 and 4 of Ref. [31] with lines 1, 2 and 3. Shown cross sections do not include absoption of p_1 in the nucleus.

Effects of the final state interaction reduce the cross section by about 40% [31].

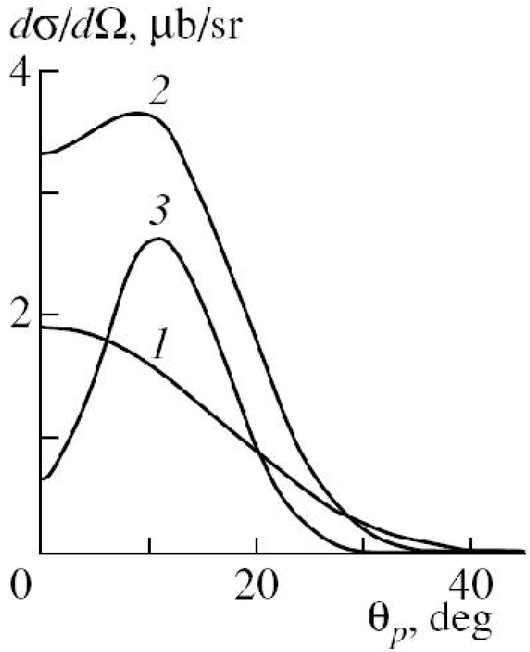

$$\gamma + A \to p_1 + {}_\eta A', \qquad A' = A - 1, \qquad (5)$$

FIG. 6: Angular distribution of protons emitted in the reaction (5) for carbon target and the final nucleus ${}_\eta A'$ in the ground state, Ref. [31]. Lines 1, 2, and 3 refer to photon beam energies of 600, 700, and 800 MeV.

Decays of η-mesic nuclei (inferred from calculations of Chiang, Oset, Liu, PRC 44, 738(1991)):

85-90%	πN	through excitation and decay of S11. This mode with back-to-back pairs was suggested by Sokol, Tryasuchev (Sov.Phys.-Lebedev Inst. Reports, 4, 31(1991)) as a trigger in seaches for η-mesic nuclei.
10-15%	NN	through excitation of S11 and its two-nucleon decay in the nuclear matter

Isotopic content (for "heavy" nuclei):

πN = 1/3 $\pi^+ n$, 1/6 $\pi^0 p$, 1/6 $\pi^0 n$, 1/3 $\pi^- p$

(due to isospin = ½)

NN = ~5% pp, ~5% nn, ~90% pn

(the latter is because the cross section of pn $\rightarrow \eta$pn (or ηd) near threshold is ~10 times bigger than the cross section of pp $\rightarrow \eta$pp)

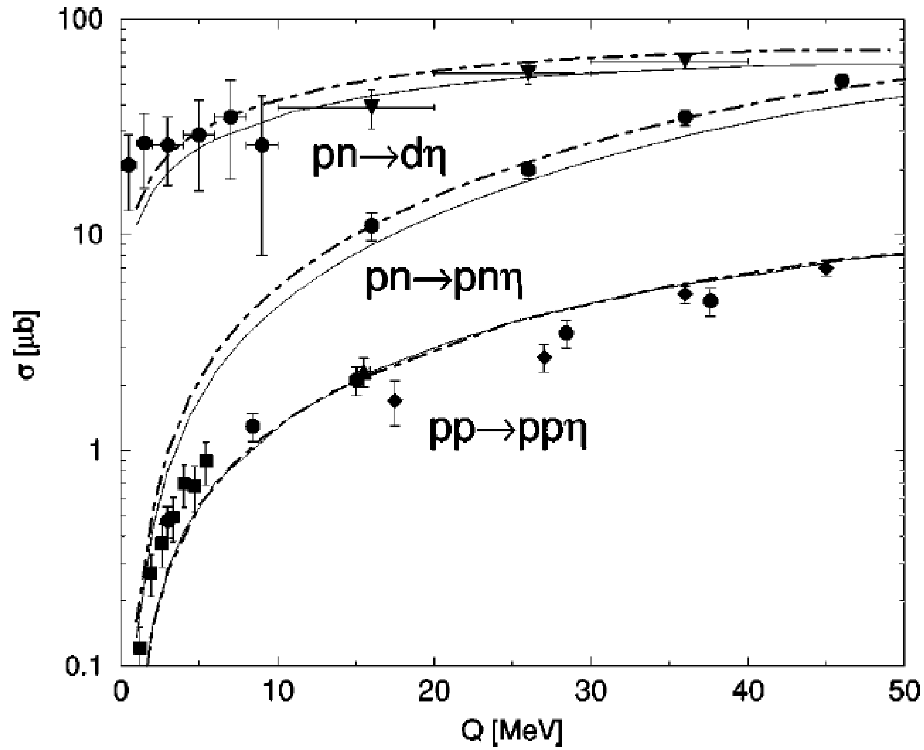

FIG. 11. Total cross sections of the reactions $pp \rightarrow pp\,\eta$, $pn \rightarrow pn\,\eta$, and $pn \rightarrow d\,\eta$ employing different NN models for the final state interaction. The solid lines represent the results with the CCF NN model [50] whereas the dashed-dotted lines were obtained for the Bonn B model [57]. The calculations are based on the extended MN model.

(borrowed from Baru et al., PRC 67, 023002 (2003)

Previous photoproduction experiments (LPI and Mainz)

LPI: Sokol et al., Part.Phys.Lett. 102, 71(2000); nucl-ex/0111020

Bremsstrahlung photon beam up to 850 MeV of the LPI electron synchrotron. Time-of-flight spectrometry.

$$\gamma + {}^{12}\mathrm{C} \;\rightarrow\; \begin{cases} p_1 + {}^{11}_{\eta}\mathrm{B} \\ n_1 + {}^{11}_{\eta}\mathrm{C} \end{cases} \;\rightarrow\; \pi^+ + n + X$$

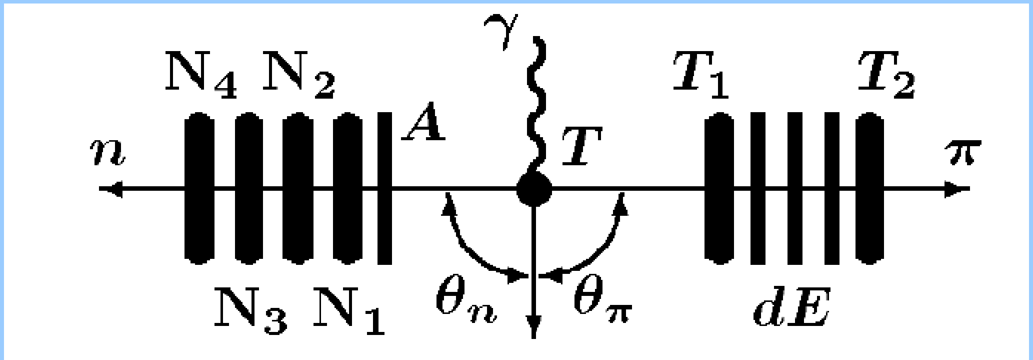

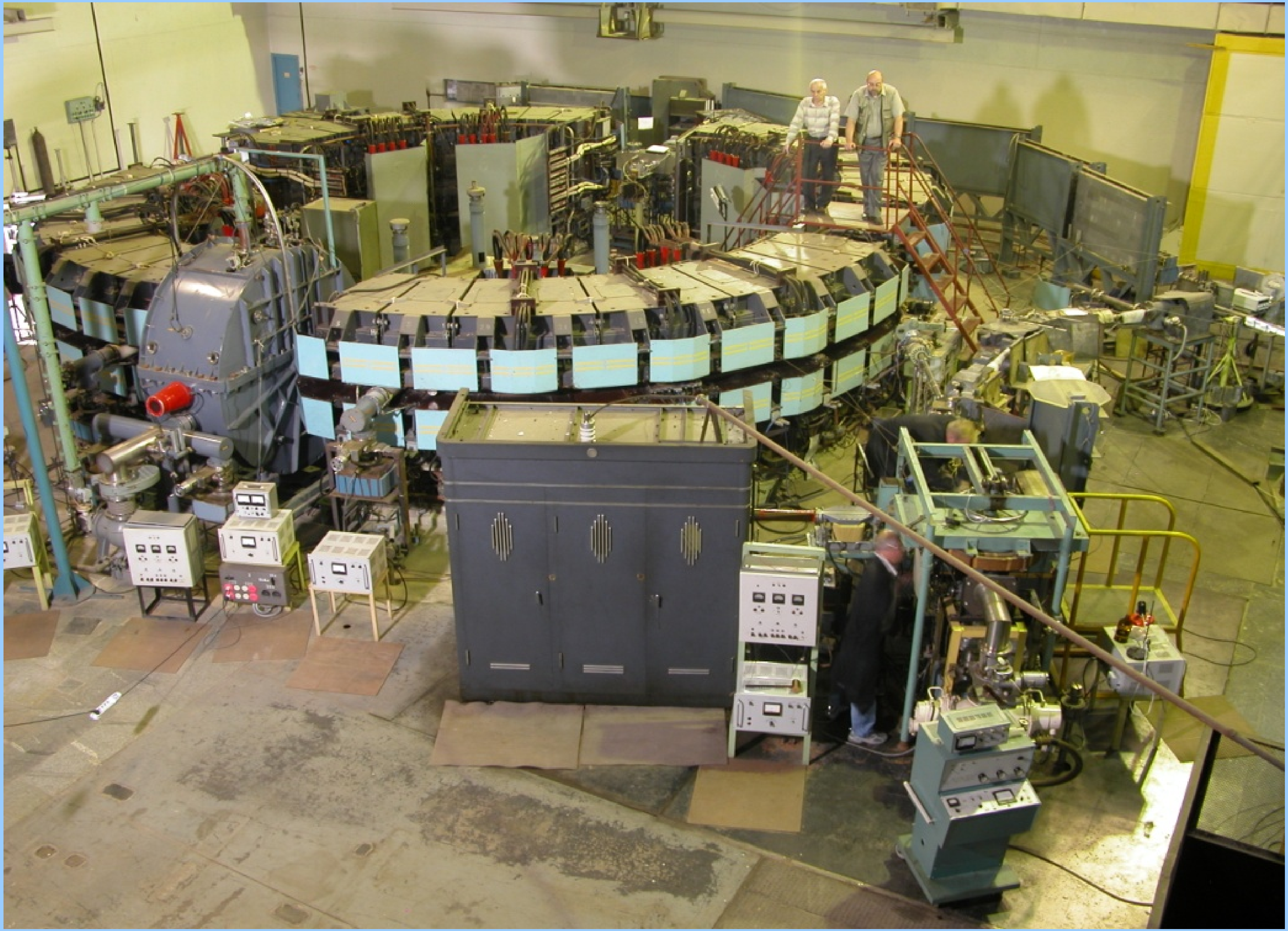

LPI 1.2-GeV electron synchrotron

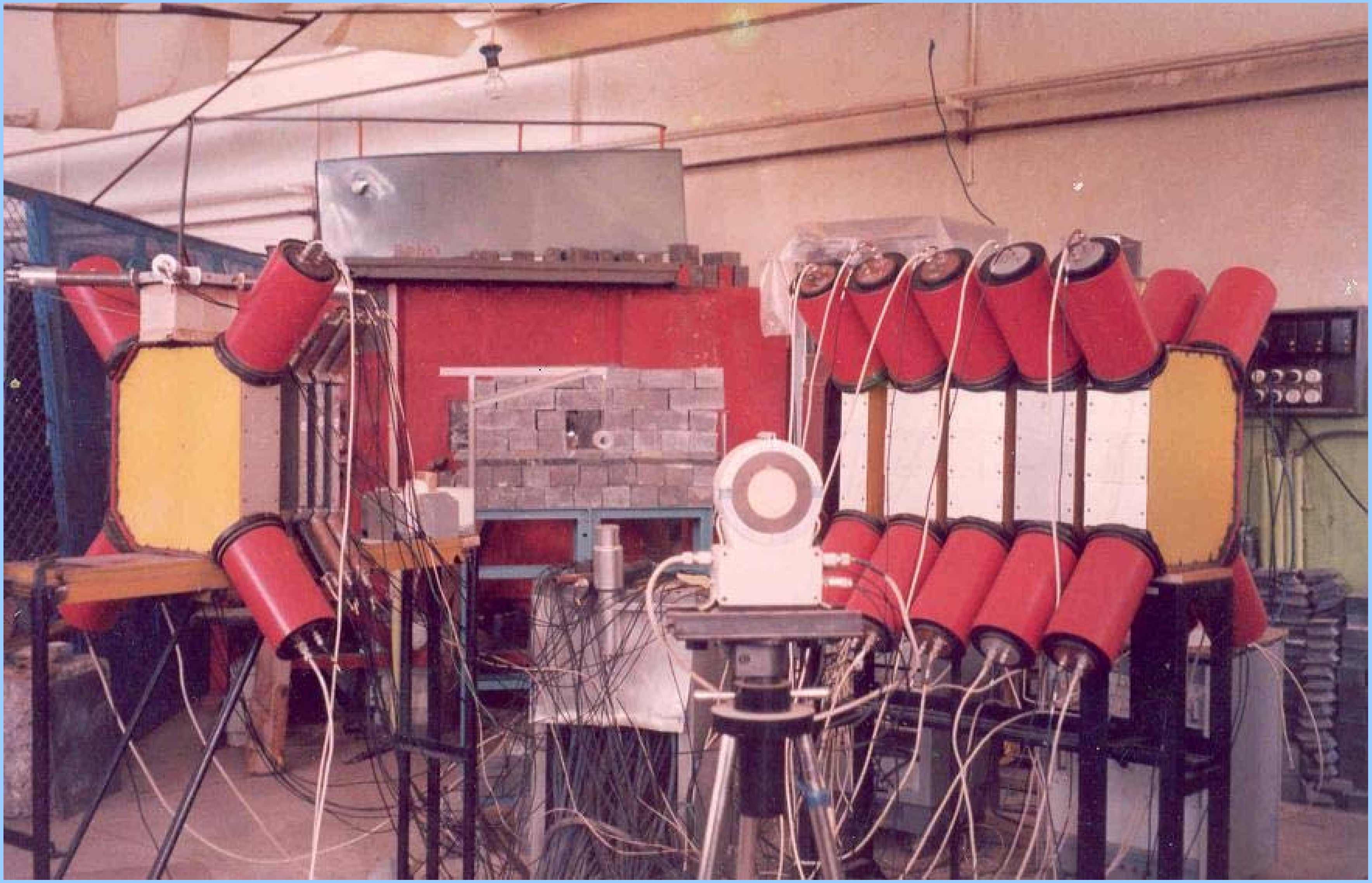

LPI experimental setup

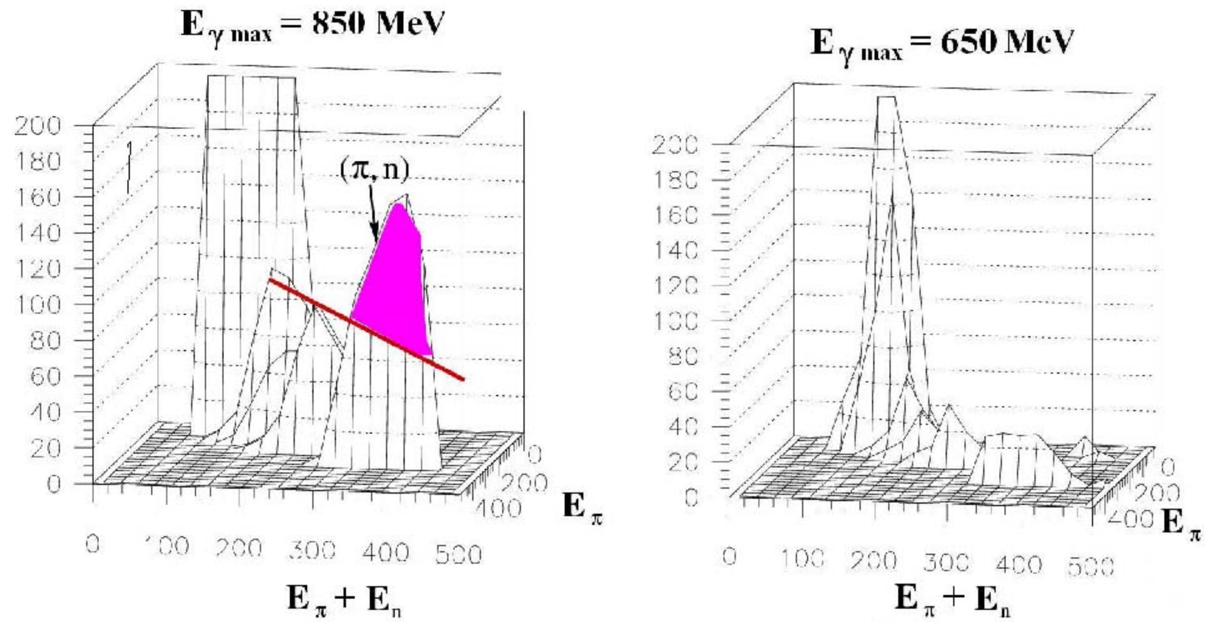

FIG. 2: Two-dimensional distributions over the kinetic energy $E_\pi + E_n$ (MeV) of the $\pi^+ n$ pair and the kinetic energy E_π (MeV) of the π^+ meson for two end-point energies $E_{\gamma\,\max}$ of the bremsstrahlung photon beam [24].

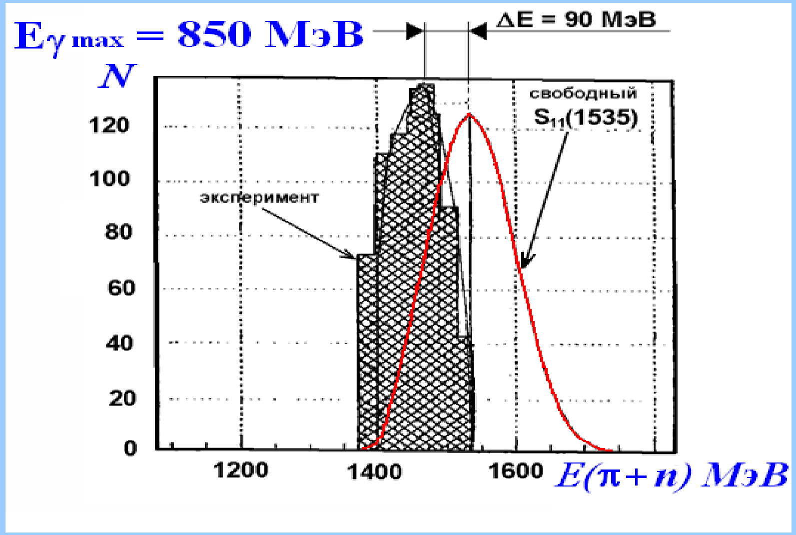

Mainz: Pfeiffer et al. PRL 92, 252001(2004)

Tagged photon beam up to 850 MeV of MAMI B.
TAPS for detection and calorimetry of π^0p.

$$\gamma + {}^3\mathrm{He} \rightarrow \pi^0 + p + X$$

(no p_1) !!

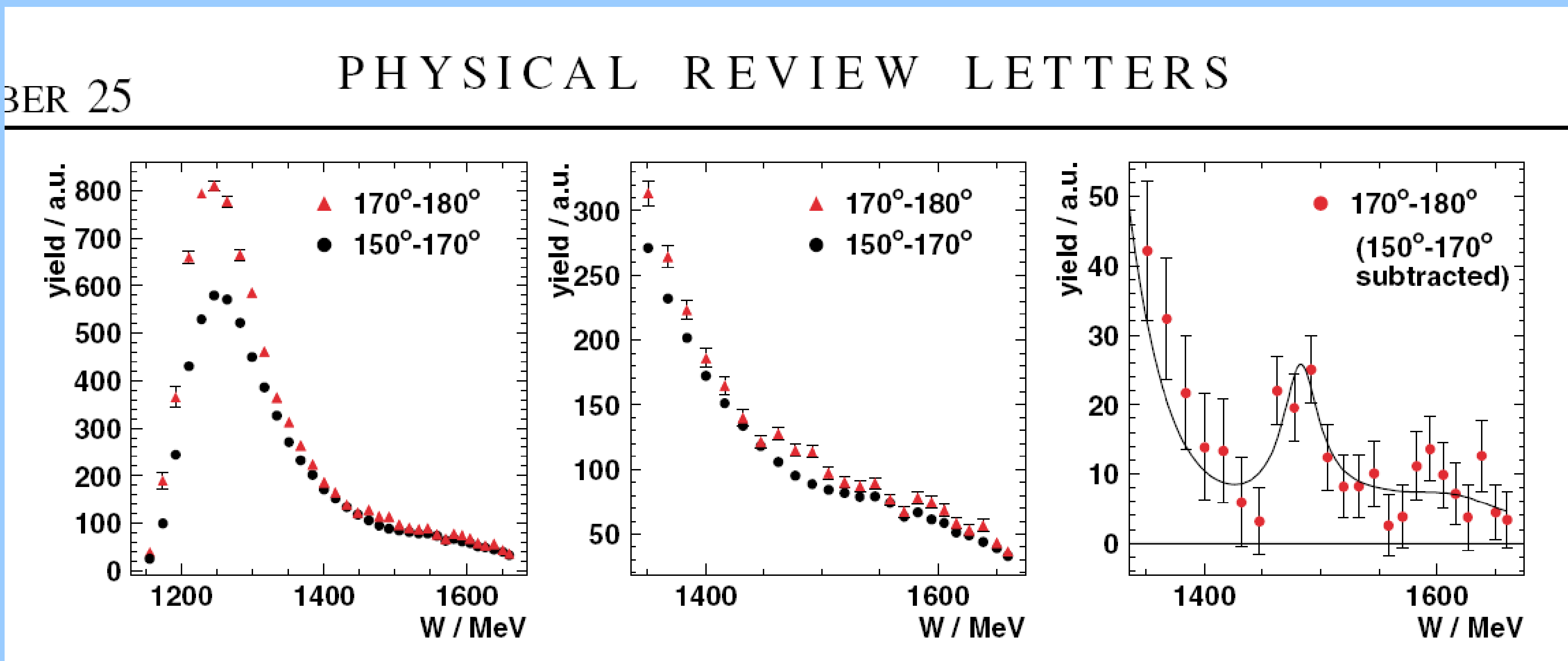

binding energy of the ${}^3_\eta$He nucleus = -4.4 ± 4.2 MeV; width = 25.6 ± 6.1 MeV

Experiment at GRAAL

$$\gamma + A \rightarrow p_1 + {}_\eta(A-1) \rightarrow p_1 + \pi^0 + p + X \rightarrow \underline{p_1 + \gamma_1 + \gamma_2 + p} + X$$

$$\gamma + A \rightarrow p_1 + {}_\eta(A-1) \rightarrow \underline{p_1 + p_2 + p_3} + X$$

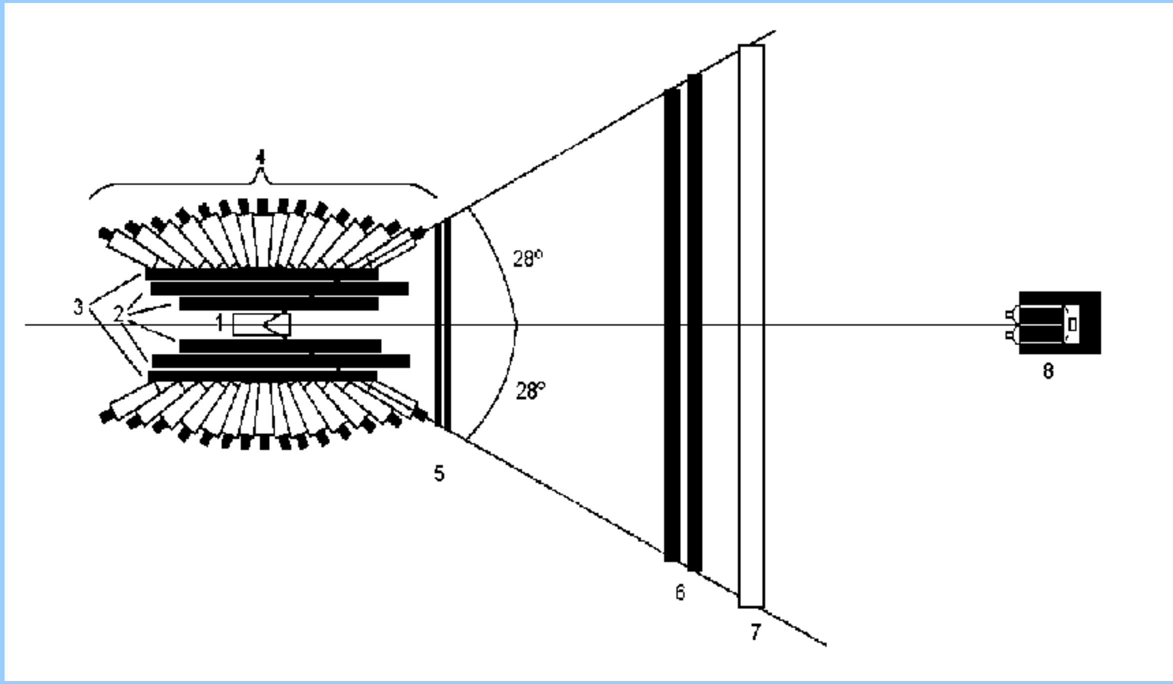

Suitable for $\gamma\gamma$pp and ppp

(what about ppn??)

Rough estimates with a “model” calorimeter

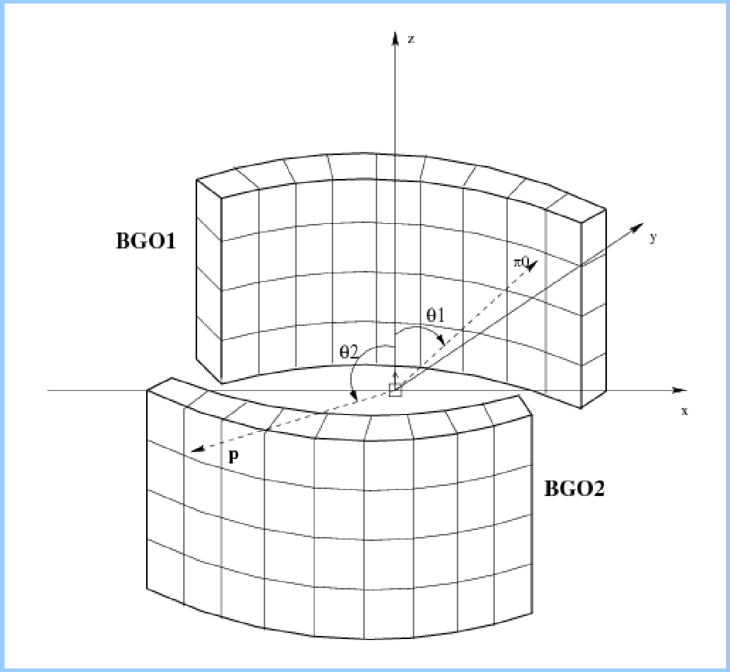

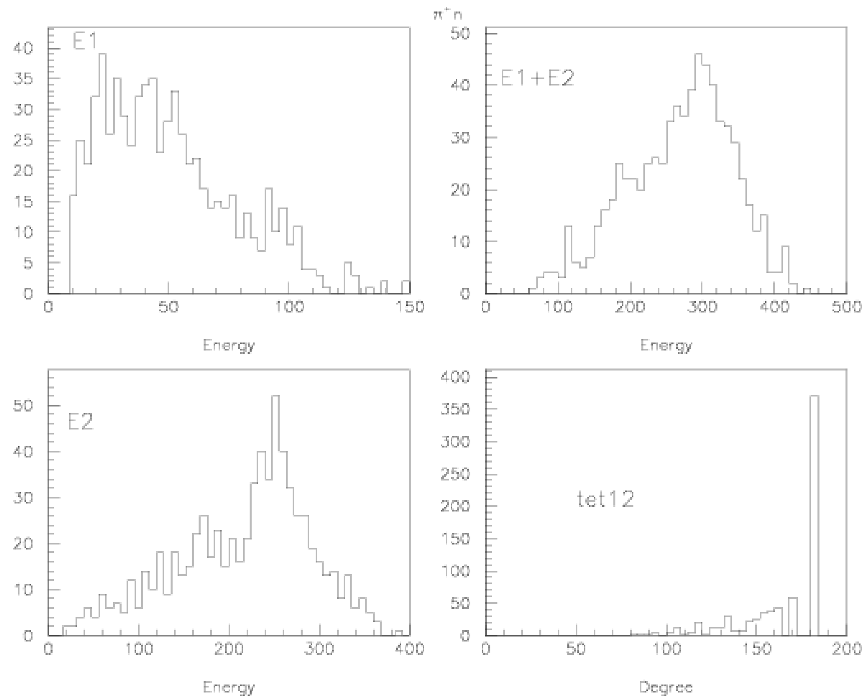

FIG. 12: Energy depositions and angular distribution of n and π^+ detected in the BGO calorimeter. Notation: $E1 = E_n$, $E2 = E_{\pi+}$, tet12 $= \theta_{n\pi+}$.

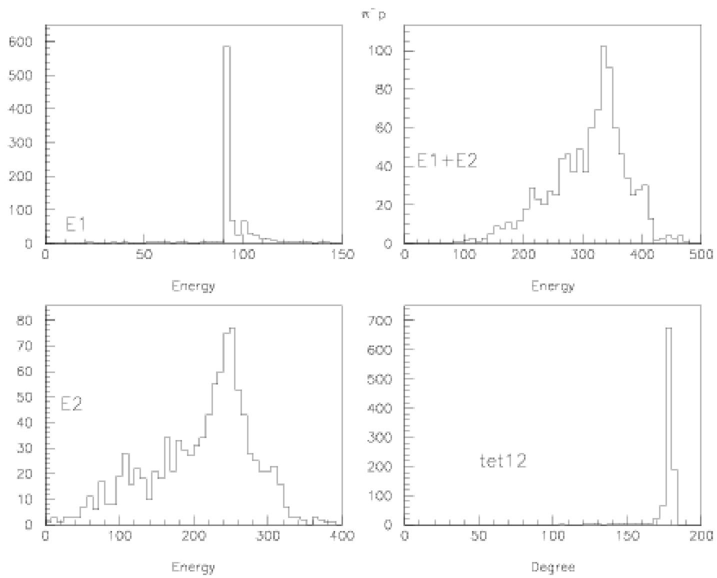

FIG. 13: Energy depositions and angular distribution of p and π^- detected in the BGO calorimeter. Notation: $E1 = E_p$, $E2 = E_{\pi^-}$, tet12 $= \theta_{p\pi^-}$.

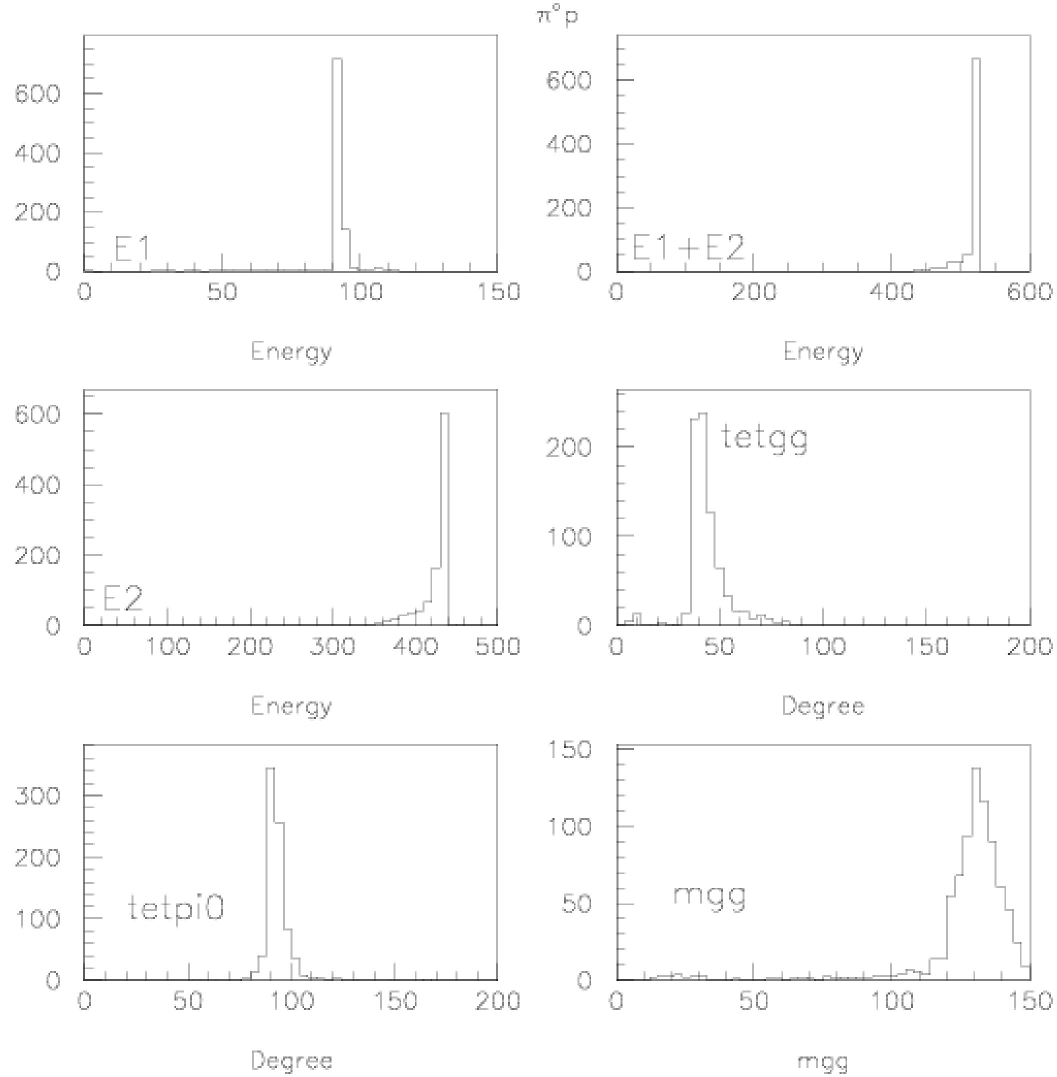

FIG. 14: Energy depositions and angular distribution of p and π^0 detected in the BGO calorimeter. Notation: $E1 = E_p$, $E2 = E_{\pi^0}$, tetgg $= \theta_{\gamma_1\gamma_2}$, tetpi0 is the reconstructed angle θ_{π^0}, and mgg is the reconstructed invariant mass $m_{\gamma_1\gamma_2}$.

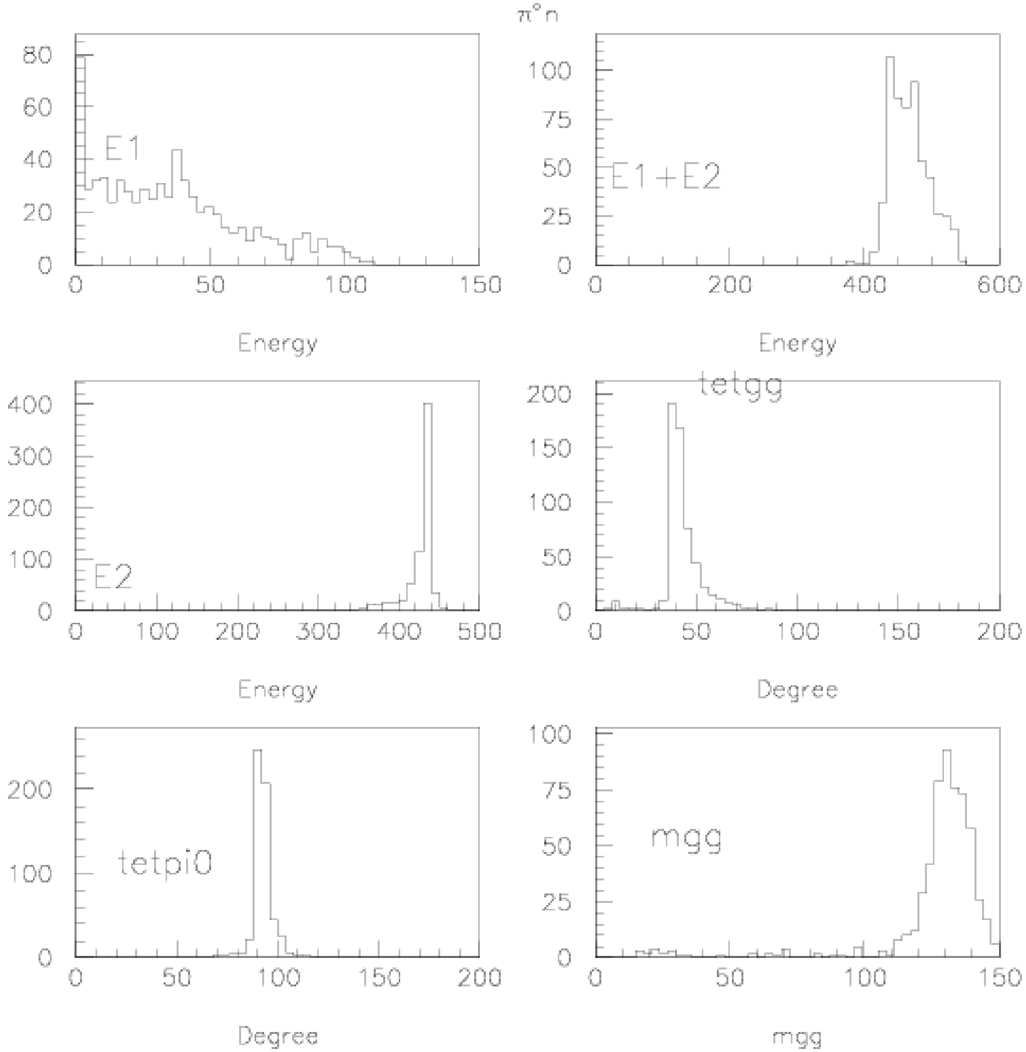

FIG. 15: Energy depositions and angular distribution of n and π^0 detected in the BGO calorimeter. Notation: $E1 = E_n$, $E2 = E_{\pi^0}$, tetgg $= \theta_{\gamma_1\gamma_2}$, tetpi0 is the reconstructed angle θ_{π^0}, and mgg is the reconstructed invariant mass $m_{\gamma_1\gamma_2}$.

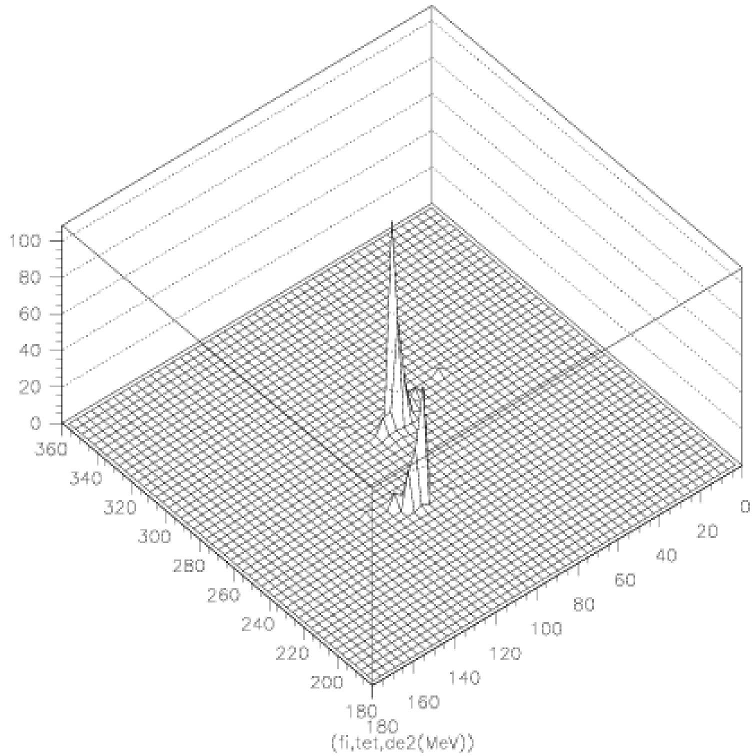

FIG. 16: The two-dimensional distribution of energy depositions over the polar and azimuthal angles, θ and ϕ, for two photons, decay products of π^0 flying from the taget at $(90^\circ, 270^\circ)$ with the energy $E_{\pi^0} = 300$ MeV.

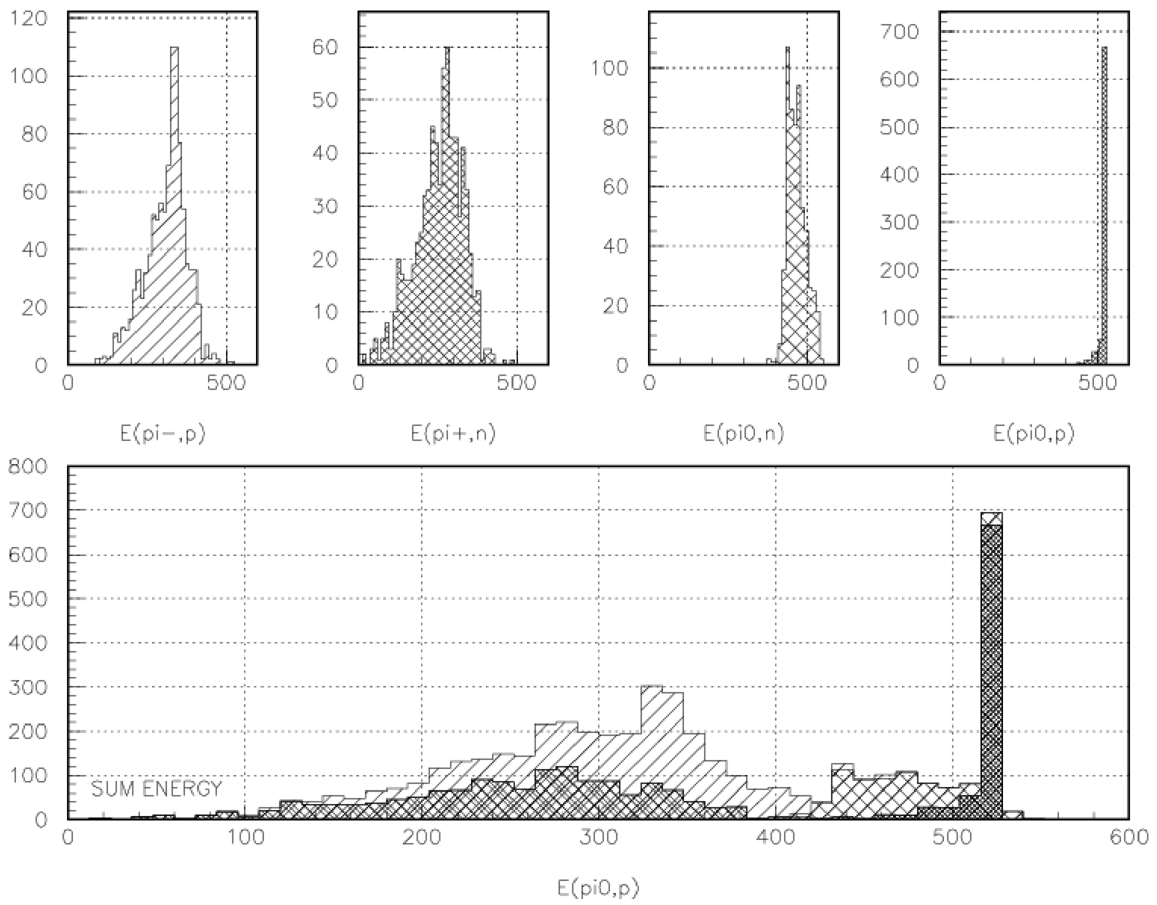

FIG. 17: Top: energy depositions of πN pairs with different charges in the BGO calorimeter. Bottom: a combined (with appropriate weights 1/3, 1/3, 1/6, 1/6) distribution which thus gives an idea of a background.

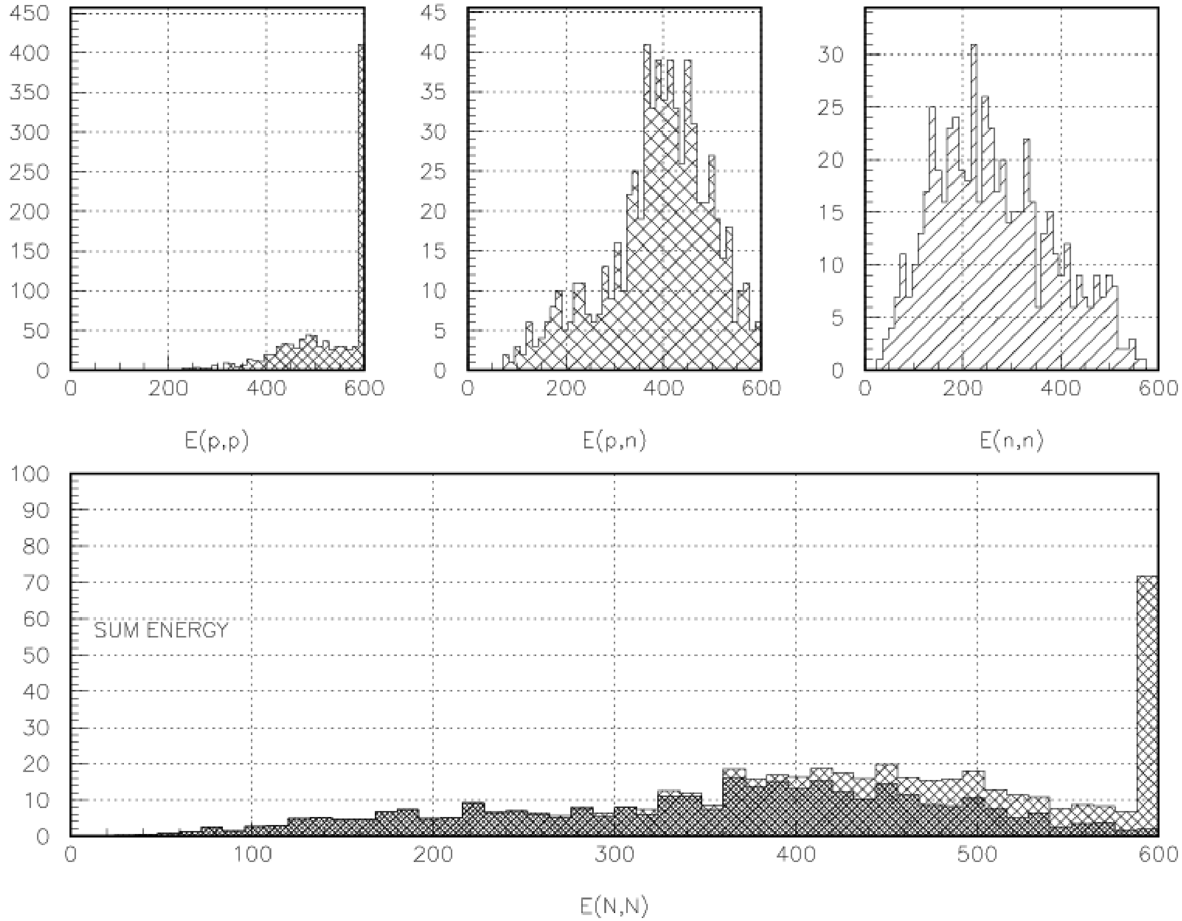

FIG. 18: Top: energy depositions of NN pairs with different charges in the BGO calorimeter. Bottom: a combined distribution (with appropriate weights 1/3, 1/3, 1/6, 1/6); it gives an idea of background.

Count rates

- The count rate of η-mesic nucleus production and decay through the coincidences $(p_1, \pi^0 p_2)$ with the carbon ($A = 12$) target is given by

$$Y(p_1, \pi^0 p_2) = \sigma_\eta(A) N_\gamma N_A \mathrm{Br}(\pi N) \mathrm{Br}(\pi^0 p \mid \pi N) \epsilon_{p_1} \epsilon_{p_2} \epsilon_{\pi^0} \sim 1000 \text{ day}^{-1}. \qquad (10)$$

Here:

$\sigma_\eta(A) \sim 2$ μb is the average total cross section of η-nucleus photoproduction in the reaction $\gamma + {}^{12}\mathrm{C} \to p_1 + {}^{11}_{\eta}\mathrm{B}$ in the energy interval $E_\gamma = 700{-}1000$ MeV; absorption of the recoil protons p_1 included here;

$N_\gamma \sim 10^6$ s^{-1} is the number of tagged photons in the same energy interval $E_\gamma = 700{-}1000$ MeV;

$N_A \simeq 4.4 \cdot 10^{23}$ cm^{-2} is the number of nuclei in the ^{12}C target of the length $l = 4$ cm;

$\mathrm{Br}(\pi N) \simeq 0.2$ is the probability of the produced η-mesic nucleus to decay to the πN channel; this probability includes two factors of ~ 0.5 and ~ 0.6 due to absorption of the pion and nucleon, respectively, emitted in the subrocess $\eta N \to \pi N$;

$\mathrm{Br}(\pi^0 p \mid \pi N) \simeq 1/6$ is the probability to have the $\pi^0 p$ final state among any possible πN pairs;

$\epsilon_{p_1} \simeq 0.8$ is the geometric efficiency to detect the recoil proton p_1 by the wire chambers and the scintillator wall;

$\epsilon_{p_2} \simeq 0.5$ is the geometric efficiency to detect a transversely emitted proton in the selected angular range $|\cos\theta_{p_2}| < 0.5$; owing to back-to-back correlations of π^0 and p_2, the geometric efficiency ϵ_{π^0} to detect the π^0-meson via its two-photon decay mode can safely be taken $\epsilon_{\pi^0} \simeq 1$;

• The count rate of η-mesic nucleus production and decay through the coincidences $(p_1, p_2 p_3)$ with the carbon $(A = 12)$ target is similarly given by

$$Y(p_1, p_2 p_3) = \sigma_\eta(A) N_\gamma N_A \mathrm{Br}(NN) \mathrm{Br}(pp \mid NN) \epsilon_{p_1} \epsilon_{p_2} \epsilon_{p_3} \sim 60 \text{ day}^{-1}. \tag{11}$$

Here:

$\mathrm{Br}(NN) \simeq 0.04$ is the probability of the produced η-mesic nucleus to decay through the NN channel; this probability includes two factors of ~ 0.6 due to absorption of nucleons in the nucleus;

$\mathrm{Br}(pp \mid NN) \simeq 0.05$ is the probability to have the pp final state among any possible NN pairs; estimating this branching ratio we take into account that the total cross section of the reverse reaction $pp \to \eta pp$ near threshold is experimentally ~ 10 times less than the total cross section of the reaction $pn \to \eta + (pn \text{ or } d)$.

Other quantities are described above with the except for the geometric efficiency for detecting the proton p_3 which, owing to back-to-back correlations between p_2 and p_3, can be taken as in the previous case: $\epsilon_{p_3} = 1$.

Conclusions

Search for η-mesic nuclei at GRAAL seems feasible with the existing apparatus (still further simulations are needed).

No large modifications are needed.

Time and energy resolutions of the setup as well as expected count rates are sufficient for obtaining valuable information on binding energies, widths, and branching ratios of light η-mesic nuclei.

^{2}H, ^{3}He, ^{4}He (?), ^{12}C (или CH_4), ^{14}N, ^{16}O (или H_2O), ^{40}Ar, ^{131}Xe, … can be used as the target.